Research Square

Preprints are preliminary reports that have not undergone peer review.
They should not be considered conclusive, used to inform clinical practice,
or referenced by the media as validated information.

Identifiability of Planar Cauchy Elasticity from Phase-Speed Data without Major Symmetry

Feng Yang

yf@zzu.edu.cn

Zhengzhou University

Research Article

Keywords: Cauchy elasticity, elastic-wave inversion, acoustic tensor, odd elasticity, material identification

Posted Date: November 5th, 2026

DOI: https://doi.org/10.21203/rs.3.rs-11135090/v1

License: This work is licensed under a Creative Commons Attribution 4.0 International License.
Read Full License

Additional Declarations: No competing interests reported.

Identifiability of Planar Cauchy Elasticity from Phase-Speed Data without Major Symmetry

Feng Yang

School of Mechanics and Safety Engineering, Zhengzhou University,
No. 100 Science Avenue, Zhengzhou 450001, China

Corresponding author: yf@zzu.edu.cn

Abstract

Acoustic identification of planar elastic moduli is well established under major symmetry. Once this symmetry is relaxed, the acoustic tensor becomes nonsymmetric and the information contained in phase speeds and polarizations changes. We determine what these two observables identify for a nine-parameter planar Cauchy-elastic law with symmetric stress. The complete phase-speed field contains only eight independent phase-speed invariants, and the associated map has generic rank eight, leaving a local one-parameter constitutive ambiguity. The six-parameter major-symmetric class occupies a lower-dimensional subset of the same eight-dimensional invariant space. Phase speeds can therefore detect departure from major symmetry for a generic anisotropic material even though they do not uniquely recover the three odd coefficients. For weak odd coupling, the phase-speed signature is quadratic whereas the polarization response is linear; special D_2, C_4, and $SO(2)$-invariant families have exactly the same phase-speed branches as certain major-symmetric materials. Polarization data, through the right eigenvectors of the acoustic tensor, supply the missing constitutive information. Two propagation directions leave one null direction in the major-symmetric part and one in the odd part, whereas three distinct directions give unique recovery. With the fourth-order stiffness Frobenius norm on constitutive space and the stacked acoustic-tensor Frobenius norm on data space, equal 60° spacing attains the sharp minimum worst-case amplification of the three-direction constitutive inverse. For experiments, phase speeds can reveal loss of major symmetry in generic anisotropy, while stable recovery of the full constitutive tensor requires polarization-resolved measurements and three suitably chosen propagation directions.

Keywords: Cauchy elasticity; elastic-wave inversion; acoustic tensor; odd elasticity; material identification.

1 Introduction

Bulk-wave measurements are widely used to identify elastic moduli because phase speeds and polarizations provide direct information about the acoustic tensor. In classical anisotropic elasticity this inverse problem is usually posed with major symmetry, $C_{ijkl} = C_{klij}$. The acoustic tensor is then symmetric, its modal polarizations are orthogonal, and classical recovery from phase velocities and polarizations is well established [1, 2, 3, 4]. Related group-velocity, stability, and measurement-angle analyses provide complementary formulations [5, 6, 7]. In two dimensions, generic uniqueness of the major-symmetric stiffness tensor has also been established from partial slowness-surface data [8].

Relaxing major symmetry changes the information content of the inverse problem. A planar nonpolar Cauchy-elastic solid with symmetric stress then has nine independent constitutive coefficients rather than six, and its acoustic tensor is generally nonsymmetric. The additional three coefficients form the major-antisymmetric, or odd, part of the stiffness tensor. Such constitutive laws have a long history in Cauchy and tensorial elasticity [9, 10, 11], and are treated in recent odd-elastic formulations [12, 13, 14, 15]. Forward analyses show that such media may exhibit nonorthogonal polarizations, mode coalescence, and polarization-dependent wave transport [16, 17, 18, 19]. The corresponding inverse problem is much less developed. It remains unclear which constitutive information is retained by phase speeds, which information requires polarization measurements, and how much directional sampling is needed once the acoustic tensor is nonsymmetric.

Phase-speed data may reveal departure from major symmetry without determining the three major-antisymmetric coefficients. We therefore treat detection and constitutive recovery separately, first identifying what is fixed by the complete phase-speed field and then what is added by polarization measurements.

The information loss is already visible in the phase-speed invariants. Each acoustic-tensor entry contains only a constant and a second angular harmonic, while the two phase-speed branches depend only on the trace and determinant of the acoustic tensor. Over all propagation directions, these quantities provide eight independent phase-speed invariants. The map from the nine constitutive coefficients to these invariants has generic rank eight, so identical phase-speed fields occur along local one-parameter families of constitutive tensors. The major-symmetric six-parameter class has generic rank six and therefore occupies a lower-dimensional subset of the full phase-speed data. A generic anisotropic material with a nonzero major-antisymmetric part can consequently be distinguished from every major-symmetric material by phase speeds alone. This distinction becomes weak near the major-symmetric limit because the leading phase-speed signature is quadratic in the odd coupling. Exact exceptions include a D_2 family with pure R^0 coupling, a C_4 pseudoscalar family, and the $SO(2)$-invariant odd solid, each with complete phase-speed fields identical to those of certain major-symmetric materials.

Polarization supplies the information that is absent from the phase-speed field. Pairing each phase speed with its measured polarization direction, i.e. the corresponding right eigenvector of the acoustic tensor, determines the acoustic tensor at that propagation angle. Two such tensors still leave two constitutive combinations unresolved: one combination of the major-symmetric coefficients and one combination of the odd coefficients. A third distinct direction removes both null directions and yields unique recovery of all nine coefficients. The placement of the three directions controls the conditioning of the constitutive interpolation, whereas the nonorthogonality of the measured polarization vectors controls the preceding reconstruction of each acoustic tensor. Equal 60° spacing attains the sharp lower bound for the complete three-direction constitutive operator with the fourth-order stiffness Frobenius norm on constitutive space and the stacked acoustic-tensor Frobenius norm on data space. The directional optimum controls the interpolation stage but does not remove the material-dependent amplification produced by nearly coalescing polarization directions.

Complete phase-speed data can test major symmetry in the generic anisotropic case, whereas full constitutive recovery requires paired polarization measurements; three suitably separated directions are then minimal. Synthetic modal-noise calculations quantify the amplification produced by directional placement and modal nonorthogonality, while redundant directions provide residuals for checking compatibility with the assumed local Cauchy law. The recovered skew-symmetric part of the acoustic tensor further constrains material symmetry, and a closed-form $SO(2)$ specialization exposes the different weak-coupling sensitivities of phase speed and polarization. The analysis concerns the bulk-wave inverse problem itself and does not assume a particular homogenized real-

ization.

2 Constitutive model and measured acoustic quantities

2.1 Planar Cauchy elasticity without major symmetry

The model is a classical planar, nonpolar Cauchy-elastic solid in the sense of Yavari and Goriely [10]: the stress is a constitutive function of strain but need not derive from a strain-energy potential. The Cauchy stress and infinitesimal strain are symmetric, so, for planar indices $i, j, k, l \in \{1, 2\}$, the elastic tensor has the minor symmetries $C_{ijkl} = C_{jikl} = C_{ijlk}$. No independent microrotation or couple stress is introduced, and the major symmetry $C_{ijkl} = C_{klij}$ is not imposed. The engineering strain and stress vectors are

$$\boldsymbol{e} = (\varepsilon_{11}, \varepsilon_{22}, 2\varepsilon_{12})^\top, \qquad \boldsymbol{s} = (\sigma_{11}, \sigma_{22}, \sigma_{12})^\top.$$

The mass density is $\varrho > 0$, and $\mathbb{C}$ denotes the physical fourth-order stiffness tensor. Its density-normalized form is $\mathbb{G} = \varrho^{-1}\mathbb{C}$. The corresponding 3×3 engineering matrix is denoted by G. To retain conventional Voigt-style stiffness labels, its nine density-normalized entries are denoted below by $C_{11}, C_{22}, C_{12}, C_{16}, C_{26}, C_{66}, R^0, K^0_a, K^0_b$; all have dimensions of squared speed. Recovery of dimensional stiffness coefficients therefore requires an independent measurement of ϱ. Consistent with established decompositions of planar tensors with only minor symmetries [11] and with recent odd-elastic formulations with symmetric Cauchy stress [14, 15], the matrix is written as

$$G = E + O, \tag{1}$$

where

$$E = \begin{pmatrix} C_{11} & C_{12} & C_{16} \\ C_{12} & C_{22} & C_{26} \\ C_{16} & C_{26} & C_{66} \end{pmatrix} \tag{2}$$

contains the six major-symmetric coefficients and

$$O = \begin{pmatrix} 0 & R^0 & K^0_a \\ -R^0 & 0 & -K^0_b \\ -K^0_a & K^0_b & 0 \end{pmatrix} \tag{3}$$

contains the three major-antisymmetric coefficients, referred to as odd coefficients in the odd-elasticity literature. The same three planar odd couplings appear in the constitutive formulations of Wolfgram and Ostoja-Starzewski [14, 15]. Their director-tensor construction identifies two anisotropic odd couplings between normal and shear components and one odd coupling between normal components. In the notation of Eq. (35) of Ref. [15], the engineering-matrix convention used here is $K^0_a = K^{0,\alpha}$ and $K^0_b = -K^{0,\beta}$; R^0 is the normal–normal odd coupling of their Eq. (36). A separate dilation-to-torque coefficient considered in the broader odd-elastic class produces nonsymmetric Cauchy stress and lies outside the class of nonpolar Cauchy-elastic solids with symmetric stress considered here.

For a propagation direction $\hat{n} = (\cos\theta, \sin\theta)$, with components $n_1 = \cos\theta$ and $n_2 = \sin\theta$, the density-normalized acoustic tensor $Q(\hat{n})$ is defined by $Q_{ik}(\hat{n}) = \mathbb{G}_{ijkl} n_j n_l$. We write $Q(\theta) \equiv Q(\hat{n}(\theta))$. Because $Q(\hat{n}) = Q(-\hat{n})$, propagation directions are parametrized by the angle θ modulo π, so $\hat{n}$ and $-\hat{n}$ represent the same measured direction. Major symmetry is the stiffness symmetry underlying Maxwell–Betti reciprocity in the present local Cauchy setting. This constitutive notion

should not be confused with propagation reciprocity: the identity $Q(\hat{n}) = Q(-\hat{n})$ makes the bulk phase-speed branches even under wave-vector reversal even when the major-antisymmetric part is nonzero. With $c_\theta = \cos\theta$ and $s_\theta = \sin\theta$,

$$Q_{11} = C_{11}c_\theta^2 + 2C_{16}c_\theta s_\theta + C_{66}s_\theta^2, \tag{4}$$

$$Q_{22} = C_{66}c_\theta^2 + 2C_{26}c_\theta s_\theta + C_{22}s_\theta^2, \tag{5}$$

$$Q_{12} = (C_{16} + K_a^0)c_\theta^2 + (C_{12} + C_{66} + R^0)c_\theta s_\theta + (C_{26} + K_b^0)s_\theta^2, \tag{6}$$

$$Q_{21} = (C_{16} - K_a^0)c_\theta^2 + (C_{12} + C_{66} - R^0)c_\theta s_\theta + (C_{26} - K_b^0)s_\theta^2. \tag{7}$$

The four component relations map the nine constitutive coefficients to the directional acoustic response.

2.2 From modal measurements to the acoustic tensor

The measurements considered below are bulk modes of a local homogeneous planar nonpolar Cauchy medium with symmetric stress and real density-normalized coefficients at one fixed working frequency. Propagation directions are identified modulo π. For polarization-resolved recovery, the acoustic tensor $Q(\theta)$ is taken to have two distinct positive real eigenvalues and a complete pair of right eigenvectors, with each polarization correctly paired with its eigenvalue. These conditions define the real-modal regime treated in the inverse analysis; plate dispersion, micropolar kinematics, odd inertia, complex effective coefficients, and unresolved branch crossings require different forward models.

At a fixed θ, the measured bulk-mode polarization directions are the directions of the right eigenvectors of Q, each understood modulo sign. Choosing unit representatives of the two polarization directions and ordering the eigenvalues as $0 < \lambda_- < \lambda_+$, write $V = (v_-, v_+)$ and $\Lambda = \mathrm{diag}(\lambda_-, \lambda_+)$. Then

$$Q(\theta) = V\Lambda V^{-1}. \tag{8}$$

For positive eigenvalues, $\lambda_\pm$ are squared phase speeds. The formula is unaffected by the sign of either eigenvector, but the pairing between each eigenvalue and its polarization must be preserved. Complex diagonalizable modal data also admit an algebraic factorization, but their experimental interpretation lies outside the present real-modal setting.

Phase-speed data alone do not determine the full nine-parameter law. In the measurement setting considered here, polarization measurements supply the right-eigenvector information needed to reconstruct Q. Introduce the four scalar acoustic combinations

$$T = Q_{11} + Q_{22}, \qquad D = Q_{11} - Q_{22}, \qquad P = Q_{12} + Q_{21}, \qquad A = \frac{Q_{12} - Q_{21}}{2}. \tag{9}$$

Here T is the trace, D the diagonal difference, P the symmetric off-diagonal sum, and A the signed scalar coefficient of the skew-symmetric part of Q. For the spectral parameter λ, the characteristic polynomial $\chi_Q(\lambda;\theta) = \det[\lambda I - Q(\theta)]$, where I is the 2×2 identity matrix, can be written

$$\chi_Q(\lambda;\theta) = \lambda^2 - T(\theta)\lambda + \frac{T(\theta)^2 - D(\theta)^2 - P(\theta)^2}{4} + A(\theta)^2. \tag{10}$$

Because T, D, P, A contain only constant and 2θ harmonics, $T(\theta)$ has three Fourier coefficients while $\det Q(\theta)$ has at most five, with harmonics 0, 2θ and 4θ. Denote the determinant coefficients by $d_0, d_{2c}, d_{2s}, d_{4c}, d_{4s}$. Hence the entire pair of phase-speed branches over all angles factors through

eight phase-speed invariants, collected in the polynomial map $\mathcal{S} : \mathbb{R}^9 \to \mathbb{R}^8$. Write the coefficient vector as $\boldsymbol{c} = (C_{11}, C_{22}, C_{12}, C_{16}, C_{26}, C_{66}, R^0, K_a^0, K_b^0)^\top$. Five distinct propagation directions modulo π already determine these eight invariants exactly in the noise-free model. Indeed, five samples determine the five coefficients of $\det Q(\theta)$, while the same samples overdetermine the three coefficients of $T(\theta)$. Thus the ten phase-speed values from five directions contain eight independent invariants and two exact redundancy relations; denser phase-speed sampling adds redundancy rather than new constitutive information.

The Jacobian of this polynomial map has rank eight on an open dense set. Here and below, "generic" refers to this regular open-dense part of the constitutive space. At $\boldsymbol{c}_\star = (4, 5, 1, 1/5, -1/5, 2, 1/5, 1/10, -1/10)^\top$, for example, the 8×8 minor obtained by deleting the C_{11} column is $13/80000 \neq 0$; Online Resource 1 verifies that the same point has two distinct positive real acoustic eigenvalues. The constant-rank theorem then gives a local one-parameter family of constitutive tensors with exactly the same phase-speed field. Figure 1(a) follows one such family by pseudo-arclength continuation. The displayed branch remains in the simple positive-real regime and stays away from the major-symmetric subspace. At singular parameter sets the constitutive ambiguity may be larger.

The phase-speed map also has an exact sign-reversal symmetry. Write $Q = Q_\mathrm{e} + Q_\mathrm{o}$, where $Q_\mathrm{e} = Q_\mathrm{e}^T$ is generated by the major-symmetric coefficient vector $\boldsymbol{c}_\mathrm{e}$ and $Q_\mathrm{o} = -Q_\mathrm{o}^T$ by the major-antisymmetric coefficient vector $\boldsymbol{c}_\mathrm{o}$. Reversing all three latter coefficients sends Q to Q^T at every angle. Therefore

$$\operatorname{spec} Q(\theta; \boldsymbol{c}_\mathrm{e}, \boldsymbol{c}_\mathrm{o}) = \operatorname{spec} Q(\theta; \boldsymbol{c}_\mathrm{e}, -\boldsymbol{c}_\mathrm{o}) \qquad \text{for every } \theta. \tag{11}$$

Here $\operatorname{spec} Q$ denotes the unordered pair of eigenvalues. Equation (11) shows directly that phase speeds are insensitive to the overall sign of the major-antisymmetric part. This discrete symmetry accounts for only part of the regular one-parameter ambiguity. Section 6 gives a stronger closed-form example in which an odd material and a major-symmetric material have identical phase speeds in every direction. Major-symmetric anisotropic media can likewise possess exceptional phase-speed-equivalent companions with different polarizations [8, 20]. In both settings, polarization contains information that the phase-speed field does not.

2.3 Information carried by phase speeds

Constitutive non-uniqueness does not preclude detection of major-symmetry breaking. To quantify the difference, compare the nine-parameter class with its six-parameter major-symmetric subspace. Let $\mathcal{E} \subset \mathbb{R}^9$ denote $\boldsymbol{c}_\mathrm{o} = 0$, and let $\mathcal{S}_\mathrm{e}$ be the restriction of the eight-component phase-speed map to $\mathcal{E}$. The classical two-dimensional major-symmetric problem is generically identifiable from sufficiently rich slowness data [8]; in the angular Fourier representation used here, the same local structure appears directly as a rank-six map. At $\boldsymbol{c}_\mathrm{e} = (4, 5, 1, 1/5, -1/5, 2)^T$, the 6×6 minor formed from $(T_0, T_c, T_s, d_0, d_{2c}, d_{2s})$ is $3/32$, so $\mathcal{S}_\mathrm{e}$ has generic rank six. The phase-speed data generated by major-symmetric materials therefore form a six-dimensional subset of the eight-dimensional data space of the full class. Where $\mathcal{S}$ has rank eight, constitutive tensors whose phase-speed fields can also be produced by a major-symmetric material form locally a codimension-two subset of the nine-parameter constitutive space. Complete phase-speed data cannot identify all nine coefficients, but they can reveal loss of major symmetry for a generic anisotropic material. This generic statement is global in the measure-theoretic sense: because $\mathcal{S}$ and $\mathcal{S}_\mathrm{e}$ are polynomial maps, the full set $\mathcal{S}^{-1}[\mathcal{S}(\mathcal{E})]$ of constitutive tensors whose phase-speed data are compatible with some major-symmetric material is contained in a measure-zero semialgebraic subset of $\mathbb{R}^9$. Online Resource 1 gives the dimension argument.

The phase-speed signature of weak odd coupling is nevertheless small. For a fixed major-symmetric part $\boldsymbol{c}_{\mathrm{e}}$ and odd direction $\boldsymbol{c}_{\mathrm{o}}$, write $\boldsymbol{c}(\varepsilon) = (\boldsymbol{c}_{\mathrm{e}}, \varepsilon \boldsymbol{c}_{\mathrm{o}})$. The quantities T, D and P are independent of ε, whereas A is linear in ε. Equation (10) therefore gives the exact expansion

$$\mathcal{S}(\boldsymbol{c}_{\mathrm{e}}, \varepsilon \boldsymbol{c}_{\mathrm{o}}) = \mathcal{S}(\boldsymbol{c}_{\mathrm{e}}, 0) + \varepsilon^2 \boldsymbol{q}(\boldsymbol{c}_{\mathrm{o}}), \tag{12}$$

where $\boldsymbol{q}$ contains only Fourier coefficients of the determinant. After allowing the nearest major-symmetric material to adjust by $O(\varepsilon^2)$, the distance from the set of spectra generated by major-symmetric materials is generically $O(\varepsilon^2)$; its leading coefficient vanishes on special families that remain phase-speed equivalent to major-symmetric materials. A dimensionless measure of distance from the major-symmetric phase-speed set can be defined without mixing the units of trace and determinant coefficients. For the observed state let $s = T_0 > 0$ and define

$$\mathcal{N}_s(T_0, T_c, T_s, d_0, d_{2c}, d_{2s}, d_{4c}, d_{4s}) = \left(\frac{T_0}{s}, \frac{T_c}{s}, \frac{T_s}{s}, \frac{d_0}{s^2}, \frac{d_{2c}}{s^2}, \frac{d_{2s}}{s^2}, \frac{d_{4c}}{s^2}, \frac{d_{4s}}{s^2} \right).$$

The normalized residual

$$\mathcal{R}_{\mathrm{MS}}(\boldsymbol{c}) = \inf_{\boldsymbol{e} \in \mathcal{E}} \left\| \mathcal{N}_s\big[\mathcal{S}(\boldsymbol{c}) - \mathcal{S}(\boldsymbol{e})\big] \right\|_2 \tag{13}$$

vanishes when the observed phase-speed data are compatible with a major-symmetric material and is generically $O(\varepsilon^2)$ for weak odd coupling. This is a deterministic distance measure; assigning a statistical detection threshold additionally requires the covariance of the measured phase-speed invariants. The quadratic scaling explains why weak major-symmetry breaking is less readily detected from phase speeds than from a first-order polarization response. The residual itself does not identify the three odd coefficients individually. Online Resource 1 gives the corresponding local codimension argument, a numerical weak odd-coupling scaling check, and a multistart numerical search for secondary major-symmetric solutions.

Exact phase-speed ambiguity remains on special families built on a square-symmetric major-symmetric base. Consider

$$C_{11} = C_{22} = \alpha, \qquad C_{12} = \gamma, \qquad C_{66} = \kappa, \qquad C_{16} = C_{26} = 0.$$

For a planar major-symmetric stiffness tensor these conditions give the square-symmetric D_4 class. Adding a pure R^0 coupling breaks the quarter-turn symmetry but retains two orthogonal mirror axes and the half-turn, giving a D_2 constitutive family; adding the pure pseudoscalar coupling $K_a^0 = K_b^0$ instead retains C_4 rotational symmetry while breaking the mirrors. In both cases a nonzero odd contribution can be absorbed into phase-speed data generated by a major-symmetric stiffness tensor.

For the square-symmetric base, then $T = \alpha + \kappa$, $D = (\alpha - \kappa)\cos 2\theta$, and $P = (\gamma + \kappa)\sin 2\theta$. For a pure R^0 coupling, $A = (R^0/2)\sin 2\theta$. If $|R^0| < |\gamma + \kappa|$, the major-symmetric material obtained by replacing γ by

$$\gamma' = \operatorname{sgn}(\gamma + \kappa)\sqrt{(\gamma + \kappa)^2 - (R^0)^2} - \kappa. \tag{14}$$

Here sgn denotes the sign function. This material has the same trace and determinant for every propagation direction. For a pure pseudoscalar coupling $K_a^0 = K_b^0 = K^0$, set $d = \alpha - \kappa$, $p = \gamma + \kappa$, and, when $|d|, |p| > 2|K^0|$,

$$a = \operatorname{sgn}(d)\sqrt{d^2 - 4(K^0)^2}, \qquad b = \operatorname{sgn}(p)\sqrt{p^2 - 4(K^0)^2}.$$

The major-symmetric coefficients

$$\alpha' = \frac{\alpha + \kappa + a}{2}, \qquad \kappa' = \frac{\alpha + \kappa - a}{2}, \qquad \gamma' = b - \kappa' \tag{15}$$

again preserve the complete phase-speed spectrum. In both constructions the odd term $4A^2$ is absorbed into $D^2 + P^2$ without changing T. These constructions show explicitly where the generic separation is lost. The $SO(2)$-isotropic ambiguity in Section 6.1 is the special case $d = p = B$ of Eq. (15).

The first three combinations in Eq. (9) describe the major-symmetric response, while A isolates the odd contribution. Because the acoustic tensor is quadratic in the direction components, each scalar contains only a constant term and a 2θ Fourier term,

$$f(\theta) = f_0 + f_c \cos 2\theta + f_s \sin 2\theta.$$

Substitution of Eqs. (4)–(7) gives

$$T_0 = \frac{C_{11} + C_{22}}{2} + C_{66}, \qquad T_c = \frac{C_{11} - C_{22}}{2}, \qquad T_s = C_{16} + C_{26}, \tag{16}$$

$$D_0 = \frac{C_{11} - C_{22}}{2}, \qquad D_c = \frac{C_{11} + C_{22}}{2} - C_{66}, \qquad D_s = C_{16} - C_{26}, \tag{17}$$

$$P_0 = C_{16} + C_{26}, \qquad P_c = C_{16} - C_{26}, \qquad P_s = C_{12} + C_{66}, \tag{18}$$

$$A_0 = \frac{K_a^0 + K_b^0}{2}, \qquad A_c = \frac{K_a^0 - K_b^0}{2}, \qquad A_s = \frac{R^0}{2}. \tag{19}$$

The directional dependence is described by twelve Fourier coefficients. A local nine-parameter planar constitutive law occupies only a nine-dimensional subspace of that coefficient space. The three remaining relations are

$$T_c = D_0, \qquad T_s = P_0, \qquad D_s = P_c. \tag{20}$$

These equalities express the fact that the twelve Fourier coefficients arise from a single local homogeneous planar Cauchy tensor.

3 Constitutive recovery from finite propagation directions

Phase speeds alone leave a constitutive ambiguity, but paired phase-speed and polarization measurements reconstruct the full acoustic tensor at each sampled angle through Eq. (8). The remaining inverse problem is then linear: how many directional acoustic tensors are needed to recover the nine constitutive coefficients, and which combinations remain invisible when the angular sampling is incomplete?

3.1 Two-direction null space

Every scalar acoustic quantity in Eq. (9) contains three angular coefficients. Two propagation directions therefore leave one harmonic combination unmeasured. In the constitutive problem this missing angular information appears as exact coefficient combinations that produce no change in either measured acoustic tensor.

For two distinct propagation directions θ_1 and θ_2, a convenient 2θ Fourier form that vanishes in both directions is

$$g(\theta) = \cos(2\theta - \theta_1 - \theta_2) - \cos(\theta_1 - \theta_2) = g_0 + g_c \cos 2\theta + g_s \sin 2\theta. \tag{21}$$

The skew-symmetric acoustic coefficient $A = \alpha_o g$ is then invisible at both directions for every scalar α_o. One odd constitutive degree of freedom therefore remains unrecoverable from two directions.

The major-symmetric subspace has an independent invisible combination. Choosing

$$T = g_0 g, \qquad D = g_c g, \qquad P = g_s g \tag{22}$$

causes all three major-symmetric response scalars to vanish at both sampled directions while still satisfying the consistency relations (20). Conversely, any major-symmetric null response is proportional to this construction. With $T = tg$, $D = dg$, and $P = pg$, the three relations in (20) reduce the coefficients to $(t, d, p) = \alpha_{\mathrm{e}}(g_0, g_c, g_s)$ for an independent scalar α_{e}. The same conclusion holds for $g_0 = 0$, which corresponds to orthogonal sampled directions.

It follows that the full two-direction measurement map has rank seven and nullity two: one combination of the major-symmetric coefficients and one combination of the odd coefficients remain acoustically invisible. The major-symmetric six-parameter problem also remains underdetermined with two propagation directions: restricting the same operator to this subspace gives rank five and nullity one. Removing major symmetry raises the two-direction nullity from one to two, while both classes still require a third distinct propagation direction.

The null-space directions are especially transparent for orthogonal measurements. If $\theta_1 = 0$ and $\theta_2 = \pi/2$, then Eq. (21) reduces to $g(\theta) = \sin 2\theta$. The major-symmetric kernel is then a pure C_{12} perturbation, while the major-antisymmetric kernel is a pure R^0 perturbation. Equations (4)–(7) show directly that neither coefficient appears in the acoustic tensors measured on the two coordinate axes. For general pairs of sampled directions these two simple null-space directions rotate into the coupled forms in Eqs. (21)–(22).

Because the unobserved combinations generate exactly zero acoustic response on both sampled directions, no post-processing of those two acoustic tensors can recover them. The missing information must come from another direction. With complete paired modal measurements in the real, diagonalizable regime, three distinct propagation directions are sufficient; the two-direction nullity also shows that three is minimal for the nine-parameter class. This exact planar rank count is the non-major-symmetric counterpart of classical limited-acoustic-data questions, where the number of recoverable major-symmetric moduli depends on the measured propagation sets and modal information [3].

3.2 Recovery from a third direction

A third distinct propagation direction supplies the remaining angular information. For any scalar constant-plus-2θ Fourier form,

$$\begin{pmatrix} f(\theta_1) \\ f(\theta_2) \\ f(\theta_3) \end{pmatrix} = M(\theta_1, \theta_2, \theta_3) \begin{pmatrix} f_0 \\ f_c \\ f_s \end{pmatrix}, \qquad M_{j\cdot} = (1, \cos 2\theta_j, \sin 2\theta_j). \tag{23}$$

Its determinant is

$$\det M = 4 \sin(\theta_1 - \theta_2) \sin(\theta_2 - \theta_3) \sin(\theta_3 - \theta_1). \tag{24}$$

Any three distinct propagation directions, with angles understood modulo π, determine the three Fourier coefficients of each of T, D, P, A. These data then determine all twelve coefficients in Eqs. (16)–(19). If the three consistency relations (20) hold, the nine constitutive coefficients follow uniquely:

$$C_{66} = \frac{T_0 - D_c}{2}, \qquad C_{11} = \frac{T_0 + D_c}{2} + T_c, \qquad C_{22} = \frac{T_0 + D_c}{2} - T_c, \tag{25}$$

$$C_{16} = \frac{T_s + D_s}{2}, \qquad C_{26} = \frac{T_s - D_s}{2}, \qquad C_{12} = P_s - C_{66}, \tag{26}$$

and

$$K_a^0 = A_0 + A_c, \qquad K_b^0 = A_0 - A_c, \qquad R^0 = 2A_s. \tag{27}$$

The third direction resolves the major-symmetric and odd angular combinations that remain acoustically invisible when only two propagation directions are measured.

4 Stability of the inverse and model checks

4.1 Choice of propagation directions

Uniqueness does not by itself ensure a stable inversion. The determinant in Eq. (24) approaches zero as two sampled propagation directions coalesce, and the angular structure of M gives a simple design rule. Its absolute value is maximized when the three propagation directions are separated by 60°,

$$\max |\det M| = \frac{3\sqrt{3}}{2} \simeq 2.598.$$

At this configuration $M^T M = \mathrm{diag}(3, 3/2, 3/2)$ up to an orthogonal rotation of the sine–cosine coefficient pair. With $\|\cdot\|_2$ denoting the spectral norm and κ_2 its associated matrix condition number,

$$\kappa_2(M) = \sqrt{2}, \qquad \|M^{-1}\|_2 = \sqrt{\frac{2}{3}}.$$

Equal spacing is the classical optimum for this scalar trigonometric interpolation problem [21], and measurement-angle sensitivity has long been recognized in ultrasonic modulus recovery [6, 7]. For the full nine-parameter problem, the same geometry also attains the optimum of the constitutive-to-acoustic operator with the fourth-order stiffness Frobenius norm on constitutive space and the stacked acoustic-tensor Frobenius norm on data space. The exact scalar constants follow from the interpolation matrix. The condition-number minimum follows from $\|M\|_F^2 = 6$ and the fixed norm of the first column. For the inverse norm, the last two columns have squared Frobenius norm 3, so their 2×2 Gram matrix has a smaller eigenvalue no larger than $3/2$; Cauchy interlacing then gives $\sigma_{\min}^2(M) \le 3/2$. The 60° design attains equality.

The interpolation result can be strengthened at the level of the complete constitutive measurement operator. Let $\mathcal{L}_\Theta$ map the nine constitutive coefficients to the three reconstructed acoustic tensors for $\Theta = (\theta_1, \theta_2, \theta_3)$. Equip the constitutive tensor with its fourth-order Frobenius norm and the data space with the norm whose square is $\sum_{j=1}^3 \|Q(\theta_j)\|_F^2$, where $\|\cdot\|_F$ denotes the Frobenius norm. For the coefficient vector $\boldsymbol{c}$ defined in Section 2, the tensor norm is $\boldsymbol{c}^T W \boldsymbol{c}$ with $W = \mathrm{diag}(1, 1, 2, 4, 4, 4, 2, 4, 4)$; these weights are the multiplicities of the engineering components in the full fourth-order tensor. The corresponding Euclidean representation under these norms is $\widetilde{\mathcal{L}}_\Theta = \mathcal{L}_\Theta W^{-1/2}$.

The constitutive domain of every three-direction measurement operator contains the isotropic major-symmetric two-parameter subspace $C_{11} = C_{22} = B + \mu$, $C_{12} = B - \mu$, $C_{66} = \mu$ and $C_{16} = C_{26} = 0$, where B and μ are the density-normalized two-dimensional bulk and shear moduli. On this subspace, $Q(\hat{n}) = \mu I + B\hat{n} \otimes \hat{n}$, so $\|\mathbb{G}\|_F^2 = 4B^2 + 8\mu^2$ and the squared three-direction data norm is $3(B^2 + 2B\mu + 2\mu^2)$, independently of the chosen directions. The two squared singular values of the normalized operator restricted to this subspace are $3/4 \pm 3\sqrt{2}/8$. With $\sigma_{\min}$ and $\sigma_{\max}$ denoting the smallest and largest singular values, every three-direction design therefore obeys

$$\sigma_{\min}^2(\widetilde{\mathcal{L}}_\Theta) \le \frac{3}{4} - \frac{3\sqrt{2}}{8}, \qquad \sigma_{\max}^2(\widetilde{\mathcal{L}}_\Theta) \ge \frac{3}{4} + \frac{3\sqrt{2}}{8}, \qquad \kappa_2(\widetilde{\mathcal{L}}_\Theta) \ge 1 + \sqrt{2}. \tag{28}$$

For 60° spacing, direct block diagonalization gives the squared singular spectrum $\{3/4 + 3\sqrt{2}/8, 9/8, 9/8, 3/4, 3/4, 3/4, 3/8, 3/8, 3/4 - 3\sqrt{2}/8\}$, so all three bounds in Eq. (28) are attained. The isotropic major-symmetric subspace sets the lower bound for every choice of propagation directions because its data norm does not depend on their orientation. Equal spacing reaches that bound without adding further worst-case directional ill-conditioning.

The distinction between the forward operator and the particular inverse used in Eqs. (26)–(27) matters away from equal spacing. Let $\widetilde{\mathcal{R}}_\Theta$ denote that closed-form reconstruction after the same invariant normalization. It is a left inverse of $\widetilde{\mathcal{L}}_\Theta$, but it need not equal the Moore–Penrose pseudoinverse. Define

$$C_\Theta^{\mathrm{LS}} = \|\widetilde{\mathcal{L}}_\Theta^\dagger\|_2, \qquad C_\Theta^{\mathrm{dir}} = \|\widetilde{\mathcal{R}}_\Theta\|_2. \tag{29}$$

Every left inverse satisfies $C_\Theta^{\mathrm{dir}} \geq C_\Theta^{\mathrm{LS}}$. At 60° spacing the two matrices are different, but both norms equal $C_\star = \sqrt{(8 + 4\sqrt{2})/3}$. Thus the closed-form inverse already attains the smallest possible worst-case amplification for the recommended design. Away from equal spacing the norms differ; for the clustered $0°, 15°, 45°$ design used below, $C_\Theta^{\mathrm{LS}} = 12.353$ whereas $C_\Theta^{\mathrm{dir}} = 13.124$. Projecting noisy acoustic data orthogonally onto the range of $\widetilde{\mathcal{L}}_\Theta$ before applying the closed-form inverse gives $\widetilde{\mathcal{R}}_\Theta \widetilde{\mathcal{L}}_\Theta \widetilde{\mathcal{L}}_\Theta^\dagger = \widetilde{\mathcal{L}}_\Theta^\dagger$; this can reduce typical errors even when the two worst-case norms coincide.

The scalar interpolation optimum is unique up to a common rotation and permutation, with propagation directions identified under $\theta \sim \theta + \pi$. Equality in the scalar interpolation bounds requires

$$\sum_{j=1}^{3} e^{2i\theta_j} = 0.$$

Three unit complex numbers with zero sum form an equilateral triple, so the angles $2\theta_j$ differ by $2\pi/3$ and the propagation directions differ by $\pi/3$. This design, uniquely optimal for scalar interpolation, also attains all bounds for the complete operator in Eq. (28).

The numerical constants in Eq. (28) depend on the chosen norms. The fourth-order Frobenius norm is invariant under physical rotation, and an isometric Kelvin/Mandel representation gives the same constants. A non-isometric Euclidean norm on engineering coefficients or a continuous-angle L^2 data norm defines a different optimization problem and may give a value different from $1 + \sqrt{2}$. Under the tensor and stacked-acoustic Frobenius norms used here, the bound is sharp. It applies to constitutive interpolation from reconstructed acoustic tensors; the preceding recovery of Q from measured eigenpairs has its own conditioning.

4.2 When the optimal directions are not admissible

The unconstrained 60° design is admissible only when all three selected propagation directions lie in the regime of two distinct positive real acoustic eigenvalues. From the symmetric part of the acoustic tensor,

$$\delta_s(\theta) = \frac{1}{2}\sqrt{D(\theta)^2 + P(\theta)^2}, \qquad \lambda_\pm(\theta) = \frac{T(\theta)}{2} \pm \sqrt{\delta_s(\theta)^2 - A(\theta)^2}.$$

Here $\delta_s(\theta)$ is half the eigenvalue splitting of the symmetric part of $Q(\theta)$. Define the admissible set

$$\mathcal{F} = \left\{ \theta \in [0, \pi) : |A(\theta)| < \delta_s(\theta), \quad \frac{T(\theta)}{2} > \sqrt{\delta_s(\theta)^2 - A(\theta)^2} \right\}.$$

A simple sufficient condition for every direction to be admissible is $\min_\theta \delta_s(\theta) > \max_\theta |A(\theta)|$ together with $\min_\theta T(\theta)/2 > \max_\theta \delta_s(\theta)$. These inequalities are not necessary; admissible directions

may also exist when either bound fails. A second sufficient condition determines when some rotated 60° triple remains admissible. Let $|\mathcal{F}^c|$ denote the angular measure of the inadmissible set in $[0, \pi)$. If

$$|\mathcal{F}^c| < \frac{\pi}{3}, \tag{30}$$

then at least one rotated 60° triple lies entirely in $\mathcal{F}$. Indeed, the integer-valued count of inadmissible members of $\{\alpha, \alpha + \pi/3, \alpha + 2\pi/3\}$ has mean $3|\mathcal{F}^c|/\pi < 1$ as α ranges over $[0, \pi)$, so it must vanish for some α. Condition (30) is sufficient rather than necessary.

If no admissible 60° triple exists, the design problem is genuinely constrained. For least-squares constitutive recovery the relevant absolute worst-case amplification is C_Θ^{LS} in Eq. (29); if the closed-form reconstruction Eqs. (26)–(27) is retained, the corresponding objective is C_Θ^{dir}. These coincide at the recommended 60° design but not for a general constrained triple. The condition number $\kappa_2(\widetilde{\mathcal{L}}_\Theta)$ remains useful when relative forward and inverse scaling are both of interest. In practice, an initial angular scan can estimate $\mathcal{F}$, after which the three-angle constrained problem is low dimensional.

4.3 Propagation of modal measurement errors

Before the directional interpolation can be applied, the acoustic tensor must be reconstructed from measured modal quantities. The conditioning of Eq. (8) therefore enters first. Sensitivity of a diagonalizable eigen-decomposition to eigenvalue and eigenvector perturbations is classical [22, 23]. Here the standard differential is written in the variables measured by the acoustic experiment. For a real diagonalizable acoustic tensor with two simple eigenvalues, let the measured eigenvalues and unit right eigenvectors differ by small increments $\delta\Lambda$ and δV, and set $\Xi = V^{-1}\delta V$. Differentiating $Q = V\Lambda V^{-1}$ gives

$$\delta Q = V\big(\delta\Lambda + [\Xi, \Lambda]\big)V^{-1} + \mathcal{O}(\eta^2), \tag{31}$$

where $[\Xi, \Lambda] = \Xi\Lambda - \Lambda\Xi$ and η denotes the size of the modal perturbation. The diagonal entries of Ξ are the components of each eigenvector perturbation along the corresponding eigenvector and commute with Λ; among eigenvector perturbations, only cross-modal mixing changes Q to first order.

Let ϕ_- and ϕ_+ be local angles of the two unit polarization directions, and let $\beta \in (0, \pi/2]$ be their acute separation. For small signed angular errors $\delta\phi_-$ and $\delta\phi_+$, direct evaluation of $V^{-1}\delta V$ gives, up to the choice of local eigenvector representatives,

$$|\Xi_{12}| = \frac{|\delta\phi_+|}{\sin\beta}, \qquad |\Xi_{21}| = \frac{|\delta\phi_-|}{\sin\beta}.$$

Writing $\Delta_\lambda = |\lambda_+ - \lambda_-|$ and using the Frobenius norm in Eq. (31) yields the first-order bound

$$\|\delta Q\|_F \le \kappa_2(V)\left[\|\delta\Lambda\|_F + \frac{\Delta_\lambda}{\sin\beta}\sqrt{(\delta\phi_-)^2 + (\delta\phi_+)^2}\right] + \mathcal{O}(\eta^2). \tag{32}$$

Nonorthogonal right eigenmodes and their coalescence are established features of odd and non-Hermitian elastodynamics [16, 17, 18]. More generally, non-Hermitian sensitivity associated with eigenvector nonorthogonality is commonly described through phase rigidity, eigenvalue condition numbers and Petermann-type factors [24]. For the present inverse problem, the same sensitivity can be written directly in the measured phase-speed and polarization variables. For two unit real right eigenvectors separated by the acute angle β, the individual eigenvalue condition number is $\csc\beta$. Reconstruction of the full acoustic tensor involves the related basis condition number $\kappa_2(V) =$

$\cot(\beta/2)$ derived below. To express this factor in measured acoustic variables, let $Q_s = (Q+Q^T)/2$ and retain $A = (Q_{12} - Q_{21})/2$ from Eq. (9). Write $m = T/2$ for the mean eigenvalue of Q_s. If $m \mp \delta_s$ are the two eigenvalues of Q_s, with $\delta_s > 0$ its half-splitting, then in an oriented eigenbasis of Q_s,

$$Q = \begin{pmatrix} m - \delta_s & A \\ -A & m + \delta_s \end{pmatrix}, \qquad \Delta_\lambda = 2\sqrt{\delta_s^2 - A^2},$$

for the simple regime of real acoustic eigenvalues $|A| < \delta_s$. A direct dot product of the normalized right eigenvectors gives

$$\cos\beta = \frac{|A|}{\delta_s}, \qquad \sin\beta = \frac{\Delta_\lambda}{2\delta_s}, \qquad \kappa_2(V) = \sqrt{\frac{\delta_s + |A|}{\delta_s - |A|}} = \cot\frac{\beta}{2}. \tag{33}$$

The columns of V are normalized to unit Euclidean length. For a two-column basis, this equal-norm scaling minimizes κ_2 over independent positive rescalings of the two eigenvectors, so the divergence in Eq. (33) cannot be removed by a more favorable normalization of the same polarization directions. Thus the factor $\Delta_\lambda/\sin\beta$ in Eq. (32) is exactly $2\delta_s$ and remains finite in the coalescence limit. The singular amplification comes from $\kappa_2(V)$: when the stiffness tensor satisfies major symmetry, Q is symmetric, $A = 0$, the polarization vectors are orthogonal, and $\kappa_2(V) = 1$, whereas $|A| \to \delta_s$ drives $\beta \to 0$ and $\kappa_2(V) \to \infty$. The same skew-symmetric acoustic component that carries the odd constitutive information can therefore degrade reconstruction of Q from measured eigenpairs as the coalescence boundary is approached.

The first-order estimate is local to a fixed pair of simple eigenvalues and is not uniform at the defective limit, where V is singular and the two polarization directions cease to provide a regular local parametrization. The perturbation formula also assumes that each eigenvalue remains paired with the corresponding eigenvector under the small perturbation. Figure 1(d) illustrates this acoustic-tensor reconstruction sensitivity directly by perturbing modal eigenvalues and polarization angles while varying $|A|/\delta_s$ at fixed Q_s. The median reconstruction error rises toward coalescence and remains below the median first-order bound from Eq. (32). Its growth is slower than $\kappa_2(V)$ because the condition number is a worst-case amplification and only part of each random perturbation aligns with the most amplified direction.

For the subsequent constitutive inversion, the full constitutive-to-acoustic operator gives a coordinate-invariant worst-case bound. The least-squares amplification $C_\Theta^{\mathrm{LS}} = \|\widetilde{\mathcal{L}}_\Theta^\dagger\|_2$ obeys

$$C_\Theta^{\mathrm{LS}} \geq C_\star = \left(\frac{3}{4} - \frac{3\sqrt{2}}{8}\right)^{-1/2} = \sqrt{\frac{8 + 4\sqrt{2}}{3}}. \tag{34}$$

Every left inverse has norm at least C_Θ^{LS}, so the same $C_\star$ is a universal lower bound for three-direction constitutive recovery with the fourth-order stiffness Frobenius norm on constitutive space and the stacked acoustic-tensor Frobenius norm on data space. At 60° spacing the closed-form inverse used here also attains $C_\star$, as shown in Section 4.1 and Online Resource 1.

Combining the constitutive-inversion bound with Eqs. (32) and (33) gives a combined local error bound directly in modal measurement errors. Let $\delta\boldsymbol{\phi}_j = (\delta\phi_{-,j}, \delta\phi_{+,j})^T$, and let V_j, $\delta_{s,j}$, and $\delta\Lambda_j$ denote the modal basis, symmetric-part half-splitting, and eigenvalue perturbation for the jth propagation direction, respectively. Let $\delta\mathbb{G}$ denote the resulting constitutive-tensor reconstruction error. Then

$$\|\delta\mathbb{G}\|_F \leq C_\star \left\{ \sum_{j=1}^{3} \kappa_2(V_j)^2 \left[\|\delta\Lambda_j\|_F + 2\delta_{s,j}\|\delta\boldsymbol{\phi}_j\|_2 \right]^2 \right\}^{1/2} + \mathcal{O}(\eta^2), \tag{35}$$

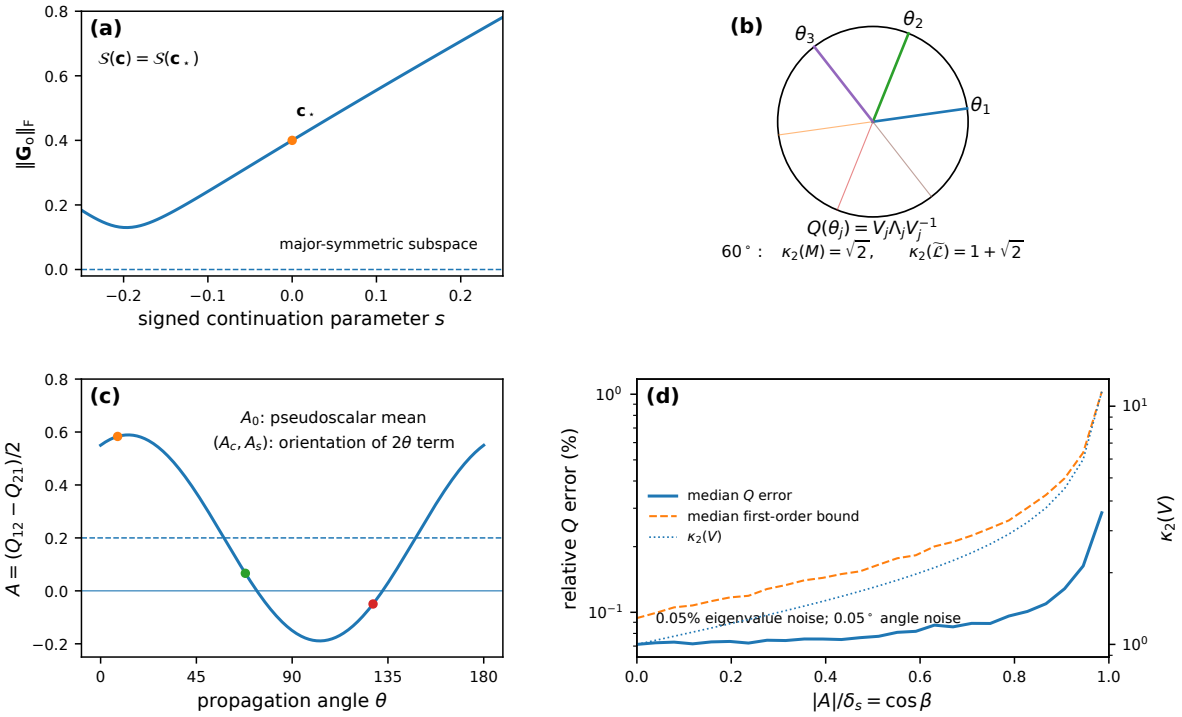


Fig. 1 Identifiability and two distinct sources of conditioning. (a) Numerical pseudo-arclength continuation of the regular constant-phase-speed level set through $\boldsymbol{c}_\star$. The ordinate is the invariant Frobenius norm of the major-antisymmetric part; zero is the major-symmetric subspace. The displayed segment retains the same phase-speed branches as $\boldsymbol{c}_\star$ and remains separated from that subspace. (b) Acoustic modal data on three propagation directions reconstruct $Q(\theta_j)$; 60° spacing gives $\kappa_2(M) = \sqrt{2}$ for the scalar interpolation and $\kappa_2(\widetilde{\mathcal{L}}_\Theta) = 1 + \sqrt{2}$ for the full constitutive-to-acoustic operator with the fourth-order stiffness Frobenius norm and the stacked acoustic-tensor Frobenius norm. (c) The skew-symmetric acoustic component separates into the pseudoscalar mean A_0 and the anisotropic 2θ coefficients (A_c, A_s). (d) With the symmetric part held fixed, synthetic noise applied to the two eigenvalues and polarization angles produces increasing reconstruction error as $|A|/\delta_s = \cos\beta$ approaches one. The dashed curve is the median first-order bound from Eq. (32); the dotted curve on the right axis is $\kappa_2(V)$.

for the equally spaced design. The directional prefactor is sharp. The modal term retains the triangle-inequality estimate of Eq. (32), so the composed bound can remain conservative. A relative constitutive-error estimate also depends on the scale of $\mathbb{G}$ and on the measurement-noise model. Orthogonal projection onto the range of the constitutive measurement operator converts the closed-form left inverse into the Moore–Penrose inverse. It may therefore reduce typical errors, even at 60° spacing where the two inverse operators have the same worst-case norm $C_\star$. The modal singularity in Eq. (33) remains present. Equal 60° spacing controls constitutive interpolation from the reconstructed acoustic tensors, whereas nearly coalescing polarization directions can still dominate the experimental sensitivity.

4.4 Redundant measurements as a model check

With $N > 3$ measured propagation directions for which the trigonometric design matrix has full column rank, each scalar quantity T, D, P, and A can be fitted to the three-dimensional basis $(1, \cos 2\theta, \sin 2\theta)$. Let $M_N \in \mathbb{R}^{N\times 3}$ be the corresponding design matrix, $\Pi_N = M_N(M_N^T M_N)^{-1} M_N^T$, let I_N denote the $N \times N$ identity, and let $\boldsymbol{y}_f$ collect the measured values for $f \in \{T, D, P, A\}$. The

four Fourier-fit residuals are

$$\mathcal{R}_f = \|(I_N - \Pi_N)\boldsymbol{y}_f\|_2, \qquad f \in \{T, D, P, A\}. \tag{36}$$

Each contributes $N-3$ residual dimensions. After fitting, the three constitutive consistency relations provide the additional residual

$$\mathcal{R}^2_{\text{cons}} = (T_c - D_0)^2 + (T_s - P_0)^2 + (D_s - P_c)^2. \tag{37}$$

The resulting discrepancy space has dimension $4(N-3)+3 = 4N-9$, exactly the difference between the $4N$ reconstructed acoustic entries and the nine-parameter constitutive model.

The two residual classes probe different departures from the constitutive model. Equation (37) uses only the major-symmetric quantities T, D, and P. Because the mapping $(A_0, A_c, A_s) \leftrightarrow (K^0_a, K^0_b, R^0)$ is a bijection, three exact directions provide no additional consistency relation involving A. With $N > 3$, the residual $\mathcal{R}_A$ instead tests the assumed angular form of the skew-symmetric acoustic component. A discrepancy confined to this component may leave $\mathcal{R}_{\text{cons}}$ essentially zero while producing a nonzero $\mathcal{R}_A$. Since the residuals share measurement uncertainty, they are not independent statistical tests unless an explicit covariance model is supplied.

4.5 Synthetic reconstruction under modal noise

To assess the combined effect of modal and constitutive conditioning, synthetic modal data were generated from known constitutive tensors, perturbed, and then inverted. Sixty admissible random nine-parameter tensors were obtained by rejection sampling around an anisotropic reference material whose symmetric acoustic part was positive definite for all directions. A candidate was retained only when every sampled propagation direction had two distinct positive real acoustic eigenvalues. The forward acoustic tensors then provided exact modal eigenvalues and right polarization directions. Independent Gaussian perturbations were applied with an eigenvalue standard deviation equal to 0.05% of the mean eigenvalue magnitude and a polarization-angle standard deviation of 0.05°. Equation (8) reconstructed the noisy acoustic tensors, after which the three-direction constitutive inversion recovered the nine constitutive coefficients. Each retained material was tested with one hundred noise realizations.

For the $0^\circ, 60^\circ, 120^\circ$ design, the median relative fourth-order-tensor error was 1.22×10^{-3} and the median first-order bound from Eq. (35) was 2.84×10^{-3}; the median bound-to-error ratio was 2.29. With the clustered set $0^\circ, 15^\circ, 45^\circ$, the median error increased to 5.61×10^{-3}. For these two designs, C^{LS}_Θ rises from 2.134 to 12.353, whereas the norm of the closed-form inverse actually used in the synthetic reconstruction, C^{dir}_Θ, rises from 2.134 to 13.124. Thus equal spacing is optimal for both inverses, while the distinction becomes visible for a constrained or clustered design. Figure 2(a,b) shows the bound comparison and the effect of directional clustering.

A separate calculation tests whether redundant measurements reveal departure from the assumed local Cauchy angular form. A pure 4θ harmonic is added to the skew-symmetric acoustic component $A(\theta)$ while T, D, P are left unchanged. The perturbation lies outside the Cauchy $0 + 2\theta$ structure and therefore provides a controlled model-mismatch signal. The same modal-noise model is used to calibrate $\mathcal{R}_A$ for twelve equally spaced additional propagation directions used to evaluate the residual. At zero added harmonic, the 95th percentile of $\mathcal{R}_A$ is 5.82×10^{-3}, or 2.59×10^{-3} after normalization by the mean acoustic eigenvalue of the reference material. On the logarithmic amplitude grid used in Fig. 2(c), the probability of exceeding this null threshold first exceeds 95% at a normalized 4θ amplitude of 2.06×10^{-3}. The resulting detection level depends on the stated angular sampling and noise model.

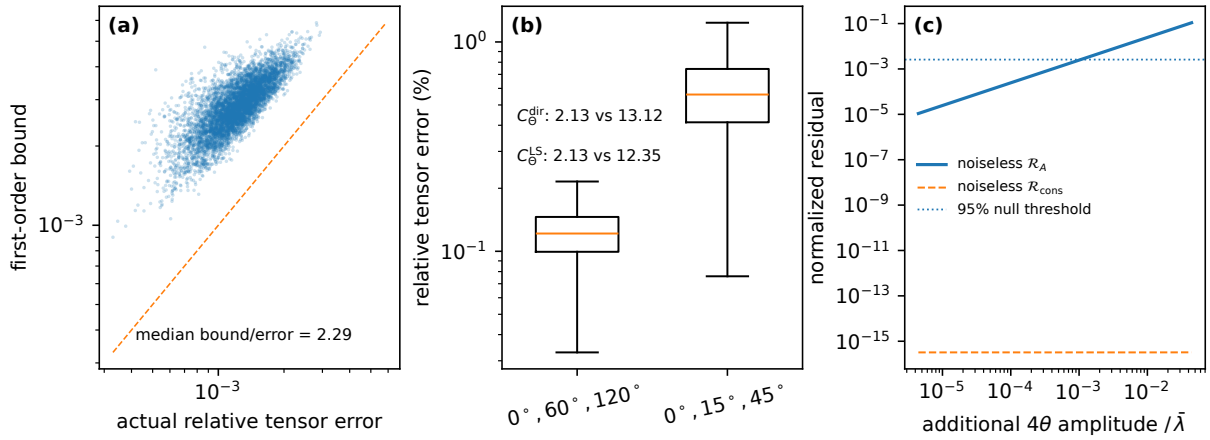


Fig. 2 Synthetic inversion and model diagnostics. (a) Actual relative fourth-order-tensor error versus the first-order bound for the equally spaced three-direction design under synthetic modal noise; the diagonal marks equality. (b) Error distributions for the equally spaced $0°, 60°, 120°$ design and the clustered $0°, 15°, 45°$ design under the same noise model; the annotations distinguish the least-squares and closed-form inverse norms. (c) Noiseless residuals produced by an additional 4θ term in $A(\theta)$, normalized by the mean acoustic eigenvalue of the reference material. The dotted line is the 95th percentile of $\mathcal{R}_A$ under the null model with the stated modal noise.

5 Material symmetry from the skew-symmetric acoustic component

Once the acoustic tensor has been reconstructed, its skew-symmetric part contains both constitutive and symmetry information. Its three Fourier coefficients recover the three odd coefficients, while their transformation under rotations and reflections constrains possible material symmetries. Acoustic criteria for symmetry planes are classical in major-symmetric elasticity [2, 25]; the same reasoning can be applied to the skew-symmetric part of the acoustic tensor when major symmetry is relaxed. From Eq. (19),

$$A(\theta) = K_a^0 \cos^2\theta + K_b^0 \sin^2\theta + \frac{R^0}{2}\sin 2\theta = A_0 + A_c \cos 2\theta + A_s \sin 2\theta. \tag{38}$$

The three Fourier coefficients of the skew-symmetric acoustic component determine the three odd coefficients. Under rotations and reflections, they separate naturally into a reflection-odd pseudoscalar part and an oriented anisotropic part.

Under a proper in-plane rotation, A_0 is invariant while (A_c, A_s) rotates through twice the physical angle, as expected for a 2θ Fourier coefficient pair. A reflection reverses the sign of the planar skew tensor. If a mirror line at angle α is a symmetry, the measured skew-symmetric component must satisfy

$$A(\theta) = -A(2\alpha - \theta)$$

for every θ. The constant part can obey this condition only when $A_0 = 0$. A nonzero

$$A_0 = \frac{K_a^0 + K_b^0}{2}$$

rules out every mirror symmetry of the full constitutive law.

When $A_0 = 0$ but $(A_c, A_s) \neq (0, 0)$, the major-antisymmetric part can still be compatible with a pair of orthogonal mirror axes. Writing the remaining 2θ term as $\mathcal{H}\cos(2\theta - \varphi)$, with $\mathcal{H} = (A_c^2 + A_s^2)^{1/2}$ and $\varphi = \operatorname{atan2}(A_s, A_c)$, where atan2 denotes the two-argument arctangent, gives

$$\alpha = \frac{1}{2}\operatorname{atan2}(A_s, A_c) + \frac{\pi}{4} \pmod{\frac{\pi}{2}}. \tag{39}$$

The major-symmetric part must possess the same reflection for that axis to be a symmetry of the full constitutive tensor.

Under cyclic fourfold rotational symmetry (C_4), $A_c = A_s = 0$, so any remaining major-antisymmetric response is purely pseudoscalar. Denote the corresponding density-normalized pseudoscalar odd modulus by K^0. In axes adapted to the fourfold structure,

$$G_{C_4} = \begin{pmatrix} C_{11} & C_{12} & K^0 \\ C_{12} & C_{11} & -K^0 \\ -K^0 & K^0 & C_{66} \end{pmatrix}, \tag{40}$$

and $A(\theta) = K^0$ is direction independent. A nonzero K^0 is compatible with C_4 rotational symmetry but excludes the mirror operations that would enlarge the symmetry group to the dihedral group D_4.

Figure 1 summarizes the inverse map, the directional design result, and the symmetry information carried by the skew-symmetric acoustic component.

6 Isotropy under proper rotations

The $SO(2)$-invariant solid provides a closed-form illustration of the different information carried by phase speed and polarization. For a planar Cauchy elastic solid with symmetric stress, proper-rotation invariance leaves two conventional moduli and one odd pseudoscalar modulus [14, 26]. A nonzero K^0 changes sign under reflection; the resulting material is therefore invariant under $SO(2)$ but not under the full orthogonal group $O(2)$. In density-normalized notation, B and μ denote the density-normalized two-dimensional bulk and shear moduli, and K^0 is the density-normalized odd modulus. In density-normalized engineering notation, the constitutive matrix is

$$G_{\text{iso}} = \begin{pmatrix} B + \mu & B - \mu & K^0 \\ B - \mu & B + \mu & -K^0 \\ -K^0 & K^0 & \mu \end{pmatrix}. \tag{41}$$

It corresponds to $C_{11} = C_{22} = B + \mu$, $C_{12} = B - \mu$, $C_{66} = \mu$, $C_{16} = C_{26} = R^0 = 0$, and $K_a^0 = K_b^0 = K^0$, so the scalar coefficient of the skew-symmetric part of the acoustic tensor is constant: $A(\theta) \equiv K^0$.

Contracting this law with the propagation direction gives, in the ordered basis $(\hat{t}, \hat{n})$ with $\hat{t} = (n_2, -n_1)$,

$$Q = \begin{pmatrix} \mu & K^0 \\ -K^0 & \mu + B \end{pmatrix}. \tag{42}$$

The mean and splitting of the two eigenvalues are $\bar{\lambda} = (\lambda_+ + \lambda_-)/2$ and $\Delta_\lambda = \lambda_+ - \lambda_- > 0$. Distinct real acoustic eigenvalues require $|B| > 2|K^0|$, which also implies $B \neq 0$. The associated nonorthogonal modes and their coalescence are part of the forward odd-elastodynamic structure already studied in the literature [16, 18, 19]; in particular, the same square-root discriminant $\sqrt{B^2 - 4(K^0)^2}$ appears explicitly in the modal spectrum of Ref. [19], whose supplementary analysis

identifies the corresponding flat-space limit. For inversion, the same relations are expressed in measured variables. The right eigenvector associated with λ_- defines the slower-mode polarization direction. Its signed inclination relative to $\hat{t}$ is denoted by ψ and taken in $(-\pi/2, \pi/2]$. Direct diagonalization gives the forward measurement relations

$$\cos 2\psi = \frac{\Delta_\lambda}{B}, \qquad \sin 2\psi = \frac{2K^0}{B}. \tag{43}$$

Solving these relations for the constitutive variables gives

$$B = \Delta_\lambda \sec 2\psi, \qquad K^0 = \frac{\Delta_\lambda}{2} \tan 2\psi, \qquad \mu = \bar{\lambda} - \frac{B}{2}. \tag{44}$$

6.1 Exact phase-speed ambiguity

The phase-speed ambiguity becomes explicit in this subclass. In the transverse–longitudinal basis, the acoustic tensor is a real 2×2 matrix whose two phase speeds depend only on its trace and determinant. Matching these two invariants therefore suffices to construct an isotropic major-symmetric representative with the same phase-speed branches. The two phase-speed invariants, $\operatorname{tr} Q = 2\mu + B$ and $\det Q = \mu(\mu + B) + (K^0)^2$, are independent of propagation direction. In the region with real acoustic eigenvalues $|B| \geq 2|K^0|$, define

$$B' = \operatorname{sgn}(B)\sqrt{B^2 - 4(K^0)^2}, \qquad \mu' = \mu + \frac{B - B'}{2}, \qquad K^{0\prime} = 0, \tag{45}$$

where sgn denotes the sign function. Then $2\mu' + B' = 2\mu + B$ and $\mu'(\mu' + B') = \mu(\mu + B) + (K^0)^2$. The major-symmetric medium $(\mu', B', 0)$ therefore has exactly the same acoustic eigenvalues as the odd medium (μ, B, K^0) for every propagation direction. When the standing positivity condition $\lambda_- > 0$ also holds, the two materials have identical phase speeds. For $B > 0$, $B' = \Delta_\lambda > 0$ and $\mu' = \lambda_- > 0$. The counterpart is then an ordinary positive-definite classical isotropic elastic solid. Equality $|B| = 2|K^0|$ gives the coalescence boundary, whereas strict inequality gives two distinct real acoustic eigenvalues. Thus, for $|B| > 2|K^0|$ with $\lambda_- > 0$, phase-speed data alone cannot determine whether the $SO(2)$-isotropic odd modulus is nonzero. The signed inclination of the polarization direction relative to the handed transverse–longitudinal frame in Eq. (43) distinguishes the odd medium from the major-symmetric material with identical phase-speed branches.

Here $\delta_s = |B|/2$ and $|A| = |K^0|$, so the general modal geometry in Eq. (33) reduces to

$$\beta = \left|\frac{\pi}{2} - 2|\psi|\right|, \qquad \frac{\Delta_\lambda}{\sin\beta} = |B|.$$

The polarization-direction angle is defined modulo π; a handed laboratory frame fixes the pseudoscalar sign convention. The limit $|\psi| \to \pi/4$ is therefore the same modal coalescence as $\beta \to 0$ in Section 4.3. The eigenvalue splitting vanishes while $\Delta_\lambda / \sin\beta$ stays finite; the singular amplification is carried by the nonorthogonality factor $\kappa_2(V)$.

6.2 Wave propagation beyond strong ellipticity

The polarization angle also encodes the sign of the density-normalized bulk modulus B:

$$B < 0 \quad \Longleftrightarrow \quad |\psi| > \frac{\pi}{4}. \tag{46}$$

For a nonsymmetric acoustic tensor, positive real eigenvalues and strong ellipticity are distinct conditions. Strong ellipticity requires the quadratic form $\boldsymbol{z}^T Q(\hat{n})\boldsymbol{z}$ to be positive for every nonzero

vector $\boldsymbol{z}$ and every propagation direction $\hat{n}$; only the symmetric part of Q contributes to this form. A nonsymmetric acoustic tensor can retain two positive real eigenvalues after its symmetric part has become indefinite. This distinction is classical in nonassociated elastoplasticity [27, 28]; the $SO(2)$-isotropic odd model expresses this boundary directly in measured wave variables.

The symmetric part of (42) has eigenvalues μ and $\mu + B$. Using (44), their product is

$$\mu(\mu + B) = \left(\bar{\lambda} - \frac{B}{2}\right)\left(\bar{\lambda} + \frac{B}{2}\right) = \bar{\lambda}^2 - \frac{B^2}{4}.$$

It is negative precisely when $\bar{\lambda} < |B|/2 = \Delta_\lambda/(2|\cos 2\psi|)$. At the same time, positivity of the smaller acoustic eigenvalue requires $\lambda_- = \bar{\lambda} - \Delta_\lambda/2 > 0$. Together, the two conditions define the following interval in measured variables:

$$\frac{\Delta_\lambda}{2} < \bar{\lambda} < \frac{\Delta_\lambda}{2|\cos 2\psi|}. \tag{47}$$

The interval has nonzero width exactly when $K^0 \neq 0$. The lower inequality is simply the positivity condition $\lambda_- > 0$, while Eq. (46) independently determines the sign of B.

Figure 3 displays this interval together with the small-$|K^0|/B$ scaling of the two measured signals. For a $B > 0$ reference within the strongly elliptic regime and $|K^0|/B \ll 1$,

$$B - \Delta_\lambda = \frac{2(K^0)^2}{B} + \mathcal{O}\left(\frac{(K^0)^4}{B^3}\right), \qquad \psi = \frac{K^0}{B} + \frac{2}{3}\left(\frac{K^0}{B}\right)^3 + \mathcal{O}\left(\frac{(K^0)^5}{B^5}\right). \tag{48}$$

For weak odd response, the change in acoustic-eigenvalue splitting is quadratic in the odd coefficient, while the polarization rotation is linear. The exact inverse also shows that the relative sensitivity to polarization-angle error alone is nonmonotone. For a small polarization-angle perturbation $\delta\psi$ at fixed Δ_λ, the induced odd-modulus perturbation δK^0 obeys

$$\frac{|\delta K^0|}{|K^0|} \simeq \frac{4|\delta\psi|}{|\sin 4\psi|}.$$

This contribution is minimized at $|\psi| = \pi/8 = 22.5^\circ$, equivalently $|K^0/B| = \sqrt{2}/4$, where its minimum value is $4|\delta\psi|$. Very weak odd response is difficult because the rotation vanishes, whereas approaching $|\psi| = 45^\circ$ is difficult because the two polarization directions coalesce. The polarization-angle contribution to the relative sensitivity is therefore minimized at this intermediate angle when Δ_λ is treated as fixed.

If σ_Δ denotes a resolution scale for the eigenvalue splitting Δ_λ (and therefore has units of squared speed) and σ_ψ denotes an angular resolution in radians, the corresponding leading-order odd-modulus scales are

$$|K^0|_\Delta \sim \sqrt{\frac{B\sigma_\Delta}{2}}, \qquad |K^0|_\psi \sim B\sigma_\psi. \tag{49}$$

These estimates describe resolution scaling. A statistical detection threshold would require an explicit noise model.

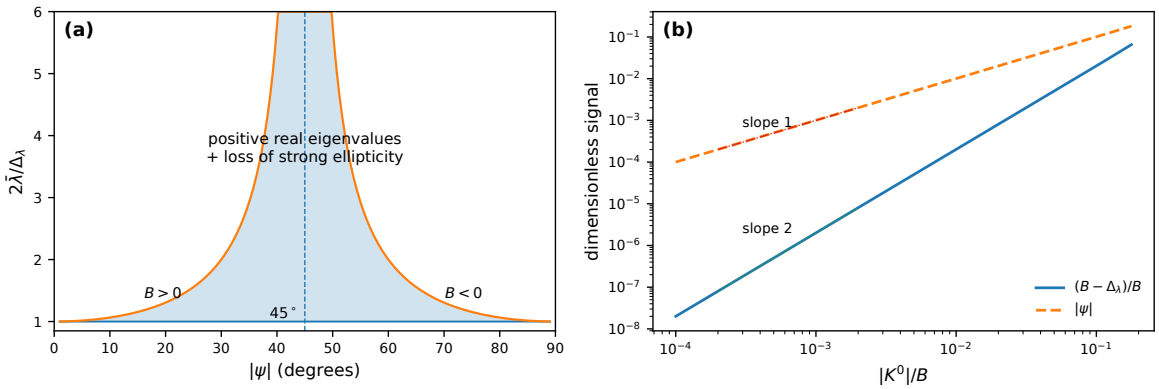


Fig. 3 Isotropy under proper rotations. (a) In measured variables, $\Delta_\lambda/2 < \bar{\lambda} < \Delta_\lambda/(2|\cos 2\psi|)$ marks the region in which the acoustic eigenvalues remain positive and real after loss of strong ellipticity; the two sides of 45° correspond to the two signs of B. (b) For a $B > 0$ reference with weak odd response, the acoustic-eigenvalue-splitting deficit is quadratic while the polarization-rotation magnitude is linear in $|K^0|/B$. The upper boundary in panel (a) is truncated at $2\bar{\lambda}/\Delta_\lambda = 6$ for display and diverges as $|\psi| \to 45°$.

7 Mechanical interpretation and measurement strategy

7.1 What the measurements determine

Phase speeds retain only the eigenvalues of the acoustic tensor. At each propagation angle they therefore determine its trace and determinant, but not the full nonsymmetric tensor. Over all angles, these data reduce to eight independent phase-speed invariants for nine constitutive coefficients. In the noise-free model, five distinct propagation directions already determine all eight invariants; additional phase-speed measurements add redundancy rather than new constitutive information. The remaining one-parameter ambiguity is therefore structural. At the same time, the six-dimensional major-symmetric class occupies only a lower-dimensional subset of the eight-dimensional phase-speed data. Loss of major symmetry is thus detectable for a generic anisotropic material even though the complete nine-parameter tensor cannot be recovered from speeds alone.

The contrast is sharper near the major-symmetric limit. Equation (12) shows that the phase-speed departure begins at second order in the odd coefficients, whereas the skew-symmetric part of the acoustic tensor and the associated polarization rotation change at first order. Polarization is therefore the more direct observable for weak major-antisymmetric coupling, while phase speeds remain useful for testing whether the measured response is compatible with major symmetry.

There are exact exceptions. The D_2 pure-R^0 construction in Eq. (14), the C_4 pseudoscalar construction in Eq. (15), and the $SO(2)$ relation in Eq. (45) all hide an odd constitutive response completely from the phase-speed field. In the $SO(2)$ case with $B > 0$, the material with identical phase-speed branches is an ordinary positive-definite isotropic elastic solid. The signed polarization inclination then provides the distinguishing information, with a linear response to weak K^0 where the eigenvalue-splitting change is only quadratic.

7.2 Measurement strategy and error sources

Once each phase speed is paired with its polarization direction, the acoustic tensor can be reconstructed for that propagation direction. Two such tensors are still insufficient: one combination of the major-symmetric coefficients and one combination of the odd coefficients remain in the exact null space. A third distinct direction removes both combinations and is therefore the minimum

required for the nine-parameter planar class. With the fourth-order stiffness Frobenius norm on constitutive space and the stacked acoustic-tensor Frobenius norm on data space, equal 60° spacing also gives the sharp optimum for the three-direction constitutive inversion. If some propagation directions fail to support two distinct positive real modes, this unconstrained design may be unavailable; the admissible set must then be identified first and the three angles chosen within it.

This directional design addresses only one source of error. Reconstruction of each individual acoustic tensor depends on the geometry of its two polarization vectors through $Q = V\Lambda V^{-1}$. When the stiffness tensor satisfies major symmetry, the vectors are orthogonal and $\kappa_2(V) = 1$. As $|A| \to \delta_s$, they coalesce and $\kappa_2(V) = \cot(\beta/2)$ diverges. No choice of propagation angles can regularize that material-dependent modal sensitivity, so an experimental uncertainty estimate must treat the modal reconstruction and the subsequent constitutive interpolation as separate stages.

The synthetic calculations in Fig. 2 follow the same sequence. The equally spaced design produces the smaller constitutive error under the stated noise model, while the first-order estimate remains conservative. With more than three directions, the extra data serve a different purpose: the Fourier-fit residuals test the assumed $0 + 2\theta$ angular form, whereas the relations in Eq. (20) test whether the fitted major-symmetric components can come from one local planar Cauchy tensor. These two residuals diagnose different departures from the model and should not be conflated.

7.3 Material symmetry, implementation, and scope

The recovered skew-symmetric acoustic component carries additional mechanical information. A nonzero mean A_0 rules out every mirror symmetry, while (A_c, A_s) selects candidate mirror axes when $A_0 = 0$; a candidate axis is a symmetry of the full constitutive tensor only if the major-symmetric part admits the same reflection. In the $SO(2)$ limit, the same measured variables also identify a regime in which the acoustic eigenvalues remain positive and real after the symmetric part of the acoustic tensor has lost positive definiteness. This is the familiar separation between wave-speed positivity and strong ellipticity for a nonsymmetric acoustic tensor, expressed here directly in measured quantities [27, 28].

An experiment must therefore resolve more than scalar travel times. The two bulk modes have to be separated, their phase speeds measured, and their polarization directions recovered. Two- or three-component scanning laser Doppler vibrometry, full-field modal imaging, and related vector displacement or velocity measurements can in principle provide these observables. Laser-based imaging has already been used for multidirectional elastic-constant reconstruction in conventional major-symmetric composites [29], while vector laser vibrometry has resolved coupled polarizations in active elastic metamaterials [30]. The present inverse formulas nevertheless require an additional modelling step: over the frequency band used for identification, the measured bulk response must be represented adequately by a local, nonpolar Cauchy elastic model with symmetric stress and approximately real effective coefficients.

Several important realizations of odd mechanics fall outside that setting. Odd-micropolar beams introduce independent rotational kinematics and frequency-dependent feedback [31]; media with odd mass density alter inertia [30]; odd plates are dispersive reduced-dimensional systems [32]. Those systems require their own forward models before the present measurement logic can be transferred. The same caution applies to complex frequency-dependent constitutive coefficients, which require complex polarization ellipses and a different modal-conditioning analysis, and to three-dimensional identification, where both the constitutive space and the acoustic eigenspaces are larger.

8 Conclusions

Removing major symmetry changes the acoustic inverse problem in a specific way. The nine-parameter planar Cauchy-elastic law with symmetric stress generates only eight independent phase-speed invariants, so even complete noise-free phase-speed data leave a one-parameter constitutive ambiguity. This does not make major-symmetry breaking invisible: the major-symmetric class occupies a lower-dimensional subset of the phase-speed data, and a generic anisotropic material outside that class can therefore be distinguished from it. The distinction becomes weak close to the major-symmetric limit because the phase-speed signature is quadratic in the odd coupling, and it disappears altogether on the exact D_2, C_4, and $SO(2)$ ambiguity families identified above. Polarization restores the missing information. Once eigenvalues and polarization vectors are paired, three distinct propagation directions are sufficient to recover all nine constitutive coefficients, whereas two directions retain one major-symmetric and one odd null direction. Equal 60° spacing gives the sharp three-direction optimum under the stated Frobenius norms, but the resulting interpolation conditioning remains separate from the singular sensitivity caused by nearly coalescing polarization vectors.

For measurement, the practical consequence is simple. Phase speeds alone can test major symmetry in generic anisotropy but cannot identify the full constitutive tensor; polarization-resolved measurements are needed for complete recovery and are also more sensitive to weak odd response. Three well-separated directions provide the minimum constitutive data, while additional directions are best used for noise reduction and model checking. These conclusions apply only over frequency ranges for which a local planar Cauchy description is an adequate representation of the measured medium.

Supplementary Information

Online Resource Supplementary derivations and numerical-validation details, including the generic rank-eight phase-speed map, the rank-six image of the major-symmetric class and weak odd-coupling scaling, explicit families with exact phase-speed ambiguity, two-direction null-space directions, conditioning of the full constitutive-to-acoustic operator, acoustic-tensor sensitivity to modal data, noise-calibrated residuals, and synthetic recovery of all constitutive coefficients.

Statements and Declarations

Funding The author declares that no funds, grants, or other support were received during the preparation of this manuscript.
Competing interests The author declares no competing interests.
Code availability The scripts used to generate the results reported in this study are provided as supplementary material in the accompanying ZIP archive.
Data availability No datasets were generated or analysed during the current study.
Author contributions Feng Yang: Conceptualization, Methodology, Formal analysis, Software, Validation, Visualization, Writing: original draft, Writing: review & editing.

References

[1] W. C. Van Buskirk, S. C. Cowin, R. Carter Jr., *A theory of acoustic measurement of the elastic constants of a general anisotropic solid*, J. Mater. Sci. **21**, 2759–2762 (1986). https://doi.org/10.1007/BF00551484

[2] A. N. Norris, *On the acoustic determination of the elastic moduli of anisotropic solids and acoustic conditions for the existence of symmetry planes*, Q. J. Mech. Appl. Math. **42**, 413–426 (1989). https://doi.org/10.1093/qjmam/42.3.413

[3] J. J. Ditri, *On the determination of the elastic moduli of anisotropic media from limited acoustical data*, J. Acoust. Soc. Am. **95**, 1761–1767 (1994). https://doi.org/10.1121/1.408695

[4] M. Mah, D. R. Schmitt, *Determination of the complete elastic stiffnesses from ultrasonic phase velocity measurements*, J. Geophys. Res. Solid Earth **108**(B1), 2016 (2003). https://doi.org/10.1029/2001JB001586

[5] A. G. Every, W. Sachse, *Determination of the elastic constants of anisotropic solids from acoustic-wave group-velocity measurements*, Phys. Rev. B **42**, 8196–8205 (1990). https://doi.org/10.1103/PhysRevB.42.8196

[6] Y. C. Chu, S. I. Rokhlin, *Stability of determination of composite moduli from velocity data in planes of symmetry for weak and strong anisotropies*, J. Acoust. Soc. Am. **95**, 213–225 (1994). https://doi.org/10.1121/1.408378

[7] C. Aristégui, S. Baste, *Optimal recovery of the elasticity tensor of general anisotropic materials from ultrasonic velocity data*, J. Acoust. Soc. Am. **101**, 813–833 (1997). https://doi.org/10.1121/1.418040

[8] M. V. de Hoop, J. Ilmavirta, M. Lassas, A. Várilly-Alvarado, *Reconstruction of anisotropic stiffness tensors from partial data around one polarization*, arXiv:2307.03312v2 (2025). https://doi.org/10.48550/arXiv.2307.03312

[9] N. I. Ostrosablin, *Symmetry classes of the anisotropy tensors of quasielastic materials and a generalized Kelvin approach*, J. Appl. Mech. Tech. Phys. **58**, 469–488 (2017). https://doi.org/10.1134/S0021894417030129

[10] A. Yavari, A. Goriely, *Nonlinear Cauchy Elasticity*, Arch. Ration. Mech. Anal. **249**, 57 (2025). https://doi.org/10.1007/s00205-025-02120-0

[11] R. Desmorat, B. Desmorat, *3D extension of Tensorial Polar Decomposition. Application to (photo-)elasticity tensors*, C. R. Mecanique **344**, 402–417 (2016). https://doi.org/10.1016/j.crme.2016.01.006

[12] C. Scheibner, A. Souslov, D. Banerjee, P. Surówka, W. T. M. Irvine, V. Vitelli, *Odd elasticity*, Nat. Phys. **16**, 475–480 (2020). https://doi.org/10.1038/s41567-020-0795-y

[13] M. Fruchart, C. Scheibner, V. Vitelli, *Odd viscosity and odd elasticity*, Annu. Rev. Condens. Matter Phys. **14**, 471–510 (2023). https://doi.org/10.1146/annurev-conmatphys-040821-125506

[14] Z. Wolfgram, M. Ostoja-Starzewski, *Scaling, anisotropy, and reciprocity of odd linear elasticity*, Int. J. Solids Struct. **338**, 114088 (2026). https://doi.org/10.1016/j.ijsolstr.2026.114088

[15] Z. Wolfgram, M. Ostoja-Starzewski, *A generalization of director tensors for odd matter in classical continuum mechanics*, Acta Mech. (2026). https://doi.org/10.1007/s00707-026-04869-1

[16] P. Gao, Y. Qu, J. Christensen, *Non-Hermitian elastodynamics in gyro-odd continuum media*, Commun. Mater. **3**, 74 (2022). https://doi.org/10.1038/s43246-022-00297-5

[17] J. Christensen, M. R. Haberman, A. Srivastava, G. Huang, G. Shmuel, *Perspective on non-Hermitian elastodynamics*, Appl. Phys. Lett. **125**, 230501 (2024). https://doi.org/10.1063/5.0224250

[18] W. Cheng, H. Qian, S. Wang, Fan Yang, Q. Wang, R. Zhu, G. Hu, G. Huang, *Elastodynamics of two-dimensional odd mechanical media: Theory, homogenization and wave characterization*, J. Mech. Phys. Solids **209**, 106502 (2026). https://doi.org/10.1016/j.jmps.2026.106502

[19] Y. Zhou, L. Tsaloukidis, J. Binysh, Y. Chen, N. Fakhri, C. Coulais, P. Surówka, *Curved Odd Elasticity*, Phys. Rev. Lett. **137**, 088301 (2026). https://doi.org/10.1103/fhwd-lmgk

[20] K. Helbig, J. M. Carcione, *Anomalous polarization in anisotropic media*, Eur. J. Mech. A/Solids **28**, 704–711 (2009). https://doi.org/10.1016/j.euromechsol.2009.02.010

[21] F. Pukelsheim, *Optimal Design of Experiments*, SIAM, Philadelphia (2006). https://doi.org/10.1137/1.9780898719109

[22] G. W. Stewart, J.-G. Sun, *Matrix Perturbation Theory*, Academic Press, Boston (1990).

[23] L. N. Trefethen, M. Embree, *Spectra and Pseudospectra: The Behavior of Nonnormal Matrices and Operators*, Princeton University Press, Princeton (2005).

[24] H. Schomerus, *Eigenvalue sensitivity from eigenstate geometry near and beyond arbitrary-order exceptional points*, Phys. Rev. Research 6, 013044 (2024). https://doi.org/10.1103/PhysRevResearch.6.013044.

[25] M. François, G. Geymonat, Y. Berthaud, *Determination of the symmetries of an experimentally determined stiffness tensor: Application to acoustic measurements*, Int. J. Solids Struct. **35**, 4091–4106 (1998). https://doi.org/10.1016/S0020-7683(97)00303-X

[26] M. Ostoja-Starzewski, P. Surówka, *Generalizing odd elasticity theory to odd thermoelasticity for planar materials*, Phys. Rev. B **109**, 064107 (2024). https://doi.org/10.1103/PhysRevB.109.064107

[27] D. Bigoni, D. Zaccaria, *Loss of strong ellipticity in non-associative elastoplasticity*, J. Mech. Phys. Solids **40**, 1313–1331 (1992). https://doi.org/10.1016/0022-5096(92)90017-V

[28] M. K. Neilsen, H. L. Schreyer, *Bifurcations in elastic-plastic materials*, Int. J. Solids Struct. **30**, 521–544 (1993). https://doi.org/10.1016/0020-7683(93)90185-A

[29] J. Zhao, J. Qiu, H. Ji, *Reconstruction of the nine stiffness coefficients of composites using a laser generation based imaging method*, Compos. Sci. Technol. **126**, 27–34 (2016). https://doi.org/10.1016/j.compscitech.2016.02.001

[30] Q. Wu, X. Xu, H. Qian, S. Wang, R. Zhu, Z. Yan, H. Ma, Y. Chen, G. Huang, *Active metamaterials for realizing odd mass density*, Proc. Natl. Acad. Sci. USA **120**, e2209829120 (2023). https://doi.org/10.1073/pnas.2209829120

[31] Y. Chen, X. Li, C. Scheibner, V. Vitelli, G. Huang, *Realization of active metamaterials with odd micropolar elasticity*, Nat. Commun. **12**, 5935 (2021). https://doi.org/10.1038/s41467-021-26034-z

[32] Y. Wang, Q. Wu, Y. Tian, G. Huang, *Non-Hermitian wave dynamics of odd plates: Microstructure design and theoretical modelling*, J. Mech. Phys. Solids **182**, 105462 (2024). https://doi.org/10.1016/j.jmps.2023.105462

Supplementary Files

This is a list of supplementary files associated with this preprint. Click to download.

- Supplementary.pdf
- scripts.zip